Experimental Performance of Robust PID Controller on a Planar Cable Robot

M. A. Khosravi and H. D. Taghirad

Abstract In this paper dynamic analysis and experimental performance of robust PID control for fully-constrained cable driven robots are studied. Since in this class of manipulators cables should remain in tension for all maneuvers in their workspace, feedback control of such robots becomes more challenging than conventional parallel robots. To overcome this problem, a corrective term is used in the proposed PID control scheme. Furthermore, in the design of PID control it is assumed that there exist bounded norm uncertainties in Jacobian matrix and in all dynamics matrices. A robust PID controller is proposed to overcome partial knowledge of robot, and to guarantee boundedness of tracking errors. Finally, the effectiveness of the proposed PID algorithm is examined through experiments and it is shown that the proposed control structure is able to provide suitable performance in practice.

1 Introduction

Cable driven parallel manipulators (CDPMs) are a special class of parallel robots in which the rigid extensible links are replaced by actuated cables. In a CDPM the end-effector is connected to the base by a number of active cables. While the cables length is changing, the end-effector is manipulated toward the desired position and orientation. Cable driven robots have some advantages compared to that of conventional robots. Using cables as an alternative to rigid links enables cable robots to be used for very large workspace applications such as large adaptive reflector and Sky-Cam [1, 2]. Because of negligible mass and inertia of cables, they are suitable for high speed applications. Moreover, they can achieve some useful properties such as

Mohammad A. Khosravi and Hamid D. Taghirad
Advanced Robotics and Automated Systems, Faculty of Electrical and Computer Engineering, K. N. Toosi University of Technology, P.O. Box 16315-1355, Tehran, Iran. e-mail: m.a.khosravi@dena.kntu.ac.ir,taghirad@kntu.ac.ir.

transportability and ease of assembly/disassembly, reconfigurability and economical structure and maintenance [3]. Consequently, CDPMs are exceptionally suitable to be used in many applications such as, handling of heavy materials [4], high speed manipulation [5, 6], cleanup of disaster areas [7], rapidly deployable rescue robots, and access to remote location and working in hazardous environment [8].

Using cables in the structure of the robot, however, introduces new challenges in the study of CDPMs. Cables can only apply tensile forces, therefore, the cables must be kept in tension in the whole workspace of the robot [9]. In order to fulfill this requirement, usually fully constrained structures are considered for a cable robot [7]. This kind of robots is being analyzed in this paper.

In comparison to the large amount of papers reported on the control of conventional robots, relatively few papers are reported on the control of CDPMs. However, many control schemes which are developed for serial or parallel robots, may be adapted for CDPMs. Lyapunov based control [10, 6], computed torque method [10, 11], sliding mode [12] and PID control [13] are some control algorithms being used in the control of CDPMs. The goal of this paper is to develop a position control algorithm based on PID, and verify its robustness against modeling uncertainties. This algorithm is formulated in the task space and uses a corrective term to ensure that all the cables remain in tension.

The structure of this paper is as follows. In section (2) kinematics and dynamics of CDPMs are studied in detail. Dynamic equations of actuators are obtained and incorporated in overall dynamics of the system. Section (3) describes the control algorithm of the system and according to upper bounds on dynamical terms, control gains are tuned such that the robust stability of the system is guaranteed. Finally, to show the effectiveness of proposed control algorithm experimental results for a planar cable driven robot are detailed in section (4).

2 Kinematics and Dynamics Analysis

2.1 Kinematics Analysis

Cable driven robot is a closed kinematic chain mechanism whose end-effector is connected to the base by a number of actuated cables. The kinematics notation of a general cable driven robot with n cables is shown in Fig. (1). In this figure $\mathbf{l}_i$ denotes the vector along i'th cable and has the same length as the cable. The length of the i'th cable is denoted by l_i. $\mathbf{S}_i$ denotes the unit vector along the i'th cable from the base to the end-effector. A_i and B_i denote the attachment points of the i'th cable on the base and end-effector, respectively. The positions of the attachment points A_i and B_i are represented by vectors $\mathbf{a}_i, \mathbf{b}_i$, respectively. Obviously, $\mathbf{a}_i$ is a constant vector in the base frame F_o and $\mathbf{b}_i$ is a constant vector in the end-effector frame F_e. The origin of the end-effector frame F_e is fixed at a reference point P, the end-effector center of mass, which is used to define the position vector of the end-effector $\mathbf{p}$. Based on

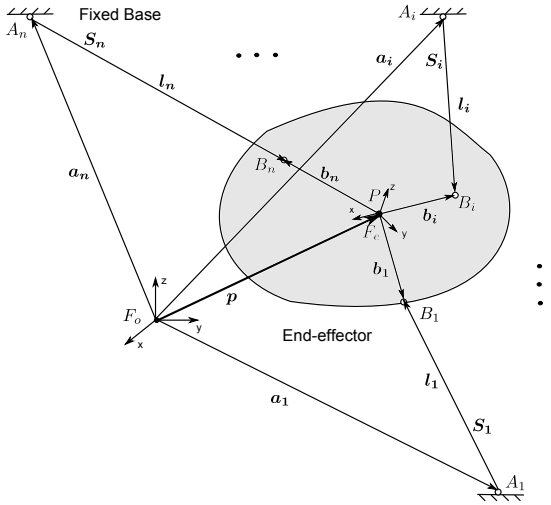

Fig. 1 Kinematic schematic of a general CDRPM.

the kinematics notation defined in Fig. (1) the position of the end-effector may be written as:

$$\mathbf{p} = \mathbf{a}_i + \mathbf{l}_i - \mathbf{b}_i \quad (i = 1, 2, \cdots, n) \tag{1}$$

where all vectors are represented in the base frame F_o. As a result

$$l_i^2 = [\mathbf{p} - \mathbf{a}_i + \mathbf{b}_i]^T \cdot [\mathbf{p} - \mathbf{a}_i + \mathbf{b}_i] \tag{2}$$

Differentiate this equation with respect to time, and rewrite it into matrix form as:

$$\dot{\mathbf{L}} = \tilde{\mathbf{J}}\mathbf{t} \tag{3}$$

in which,

$$\tilde{\mathbf{J}} = \begin{bmatrix} \mathbf{S}_1 & \mathbf{S}_2 & \cdots & \mathbf{S}_n \\ \mathbf{b}_1 \times \mathbf{S}_1 & \mathbf{b}_2 \times \mathbf{S}_2 & \cdots & \mathbf{b}_n \times \mathbf{S}_n \end{bmatrix}^T \tag{4}$$

and, $\dot{\mathbf{L}} = \left[\dot{l}_1, \dot{l}_2, \cdots, \dot{l}_n\right]^T$, and $\mathbf{t} = [\dot{\mathbf{p}}, \boldsymbol{\omega}]^T = [\dot{p}_x, \dot{p}_y, \dot{p}_z, \omega_x, \omega_y, \omega_z]^T$. The matrix $\tilde{\mathbf{J}}$ is the Jacobian matrix corresponding to the general cable robot, $\dot{\mathbf{p}}$ denotes the velocity vector of point P; $\boldsymbol{\omega}$ denotes angular velocity of the end-effector, and $\mathbf{t}$ represents the twist vector in $\mathbb{R}^6$, which consists of the linear and angular velocities of the end-effector.

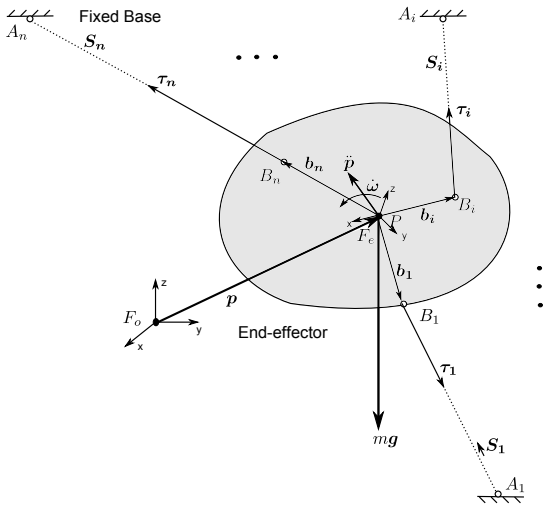

Fig. 2 Dynamics schematic of a general CDRPM.

2.2 Dynamics Analysis

For a typical cable robot the mass of the cables is extremely smaller than that of the end-effector, and can therefore be neglected. By this assumption the dynamics model of the robot reduces to that of the end-effector. Based on the dynamics notation given in Fig. (2), when all the cables are in tension the equations of motion can be derived using Newton-Euler laws [14].

$$\begin{bmatrix} m\mathbf{I} & \mathbf{0}_{3\times3} \\ \mathbf{0}_{3\times3} & \mathbf{I}_P \end{bmatrix} \begin{bmatrix} \ddot{\mathbf{p}} \\ \dot{\boldsymbol{\omega}} \end{bmatrix} + \begin{bmatrix} \mathbf{0}_{3\times1} \\ \boldsymbol{\omega} \times \mathbf{I}_P \boldsymbol{\omega} \end{bmatrix} + \begin{bmatrix} -m\mathbf{g} \\ \mathbf{0}_{3\times1} \end{bmatrix} = -\tilde{\mathbf{J}}^T \boldsymbol{\tau} \tag{5}$$

in which, m denotes mass of the end-effector; $\mathbf{I}_P$ denotes inertia tensor of the end-effector about point P in F_o frame; $\mathbf{g}$ denotes the gravity acceleration vector; $\boldsymbol{\tau} = [\tau_1, \tau_2, \cdots, \tau_n]$ denotes the vector of cable forces and τ_i denotes the cable force value in the i'th cable.

Consider $\mathbf{x} = [x_p, y_p, z_p, \alpha, \beta, \gamma]^T$ as generalized coordinates vector, in which $\boldsymbol{\theta} = [\alpha, \beta, \gamma]^T$ is the vector of Euler angles. With this definition the rotation matrix ${}^{F_o}\mathbf{R}_{F_e}$ can be written in term of roll-pitch-yaw Euler angels,

$${}^{F_o}\mathbf{R}_{F_e} = \begin{bmatrix} c\beta c\gamma & c\gamma s\alpha s\beta - c\alpha s\gamma & c\alpha c\gamma s\beta + s\alpha s\gamma \\ c\beta s\gamma & c\alpha c\gamma + s\alpha s\beta s\gamma & -c\gamma s\alpha + c\alpha s\beta s\gamma \\ -s\beta & c\beta s\alpha & c\alpha c\beta \end{bmatrix} \tag{6}$$

where c and s denotes shorthand writings for sin and cos functions, respectively. Furthermore, the angular velocity of the end-effector can be written as,

$$\boldsymbol{\omega} = \mathbf{E}\dot{\boldsymbol{\theta}} \quad , \quad \dot{\boldsymbol{\theta}} = \left[\dot{\alpha}, \dot{\beta}, \dot{\gamma}\right]^T \tag{7}$$

in which,

$$\mathbf{E} = \begin{bmatrix} c\beta c\gamma & -s\gamma & 0 \\ c\beta s\gamma & c\gamma & 0 \\ -s\beta & 0 & 1 \end{bmatrix}$$

Thus, one can write,

$$\dot{\mathbf{L}} = \mathbf{J}\dot{\mathbf{x}} \tag{8}$$

in which,

$$\mathbf{J} = \tilde{\mathbf{J}} \begin{bmatrix} \mathbf{I}_{3\times3} & \mathbf{0}_{3\times3} \\ \mathbf{0}_{3\times3} & \mathbf{E} \end{bmatrix} \tag{9}$$

With this notation, the equations of motion can be written in the terms of $\mathbf{x}$. After some manipulation these equations can be derived in an explicit form as,

$$\mathbf{M}(\mathbf{x})\ddot{\mathbf{x}} + \mathbf{C}(\mathbf{x},\dot{\mathbf{x}})\dot{\mathbf{x}} + \mathbf{G}(\mathbf{x}) = -\mathbf{J}^T\boldsymbol{\tau} \tag{10}$$

in which,

$$\mathbf{M}(\mathbf{x}) = \begin{bmatrix} m\mathbf{I}_{3\times3} & \mathbf{0}_{3\times3} \\ \mathbf{0}_{3\times3} & \mathbf{E}^T\mathbf{I}_P\mathbf{E} \end{bmatrix} \tag{11}$$

$$\mathbf{C}(\mathbf{x},\dot{\mathbf{x}}) = \begin{bmatrix} \mathbf{0}_{3\times3} & \mathbf{0}_{3\times3} \\ \mathbf{0}_{3\times3} & \mathbf{E}^T\mathbf{I}_P\dot{\mathbf{E}} + \mathbf{E}^T(\mathbf{E}\dot{\boldsymbol{\theta}})_\times\mathbf{I}_P\mathbf{E} \end{bmatrix} \tag{12}$$

$$\mathbf{G}(\mathbf{x}) = \begin{bmatrix} -m\mathbf{g} \\ \mathbf{0}_{3\times1} \end{bmatrix} \tag{13}$$

2.3 Overall Robot Dynamics

In this section overall dynamics of the cable robot considering actuators dynamics is obtained. In practice a robot is always experiencing friction and disturbance forces. Therefore, we can reformulate the manipulator dynamics as

$$\mathbf{M}(\mathbf{x})\ddot{\mathbf{x}} + \mathbf{C}(\mathbf{x},\dot{\mathbf{x}})\dot{\mathbf{x}} + \mathbf{G}(\mathbf{x}) + \mathbf{F}_d\dot{\mathbf{x}} + \mathbf{F}_s(\dot{\mathbf{x}}) + \mathbf{T}_d = -\mathbf{J}^T\boldsymbol{\tau} \tag{14}$$

with $\mathbf{x}$ as the generalized coordinates vector, $\boldsymbol{\tau}$ as the vector of cable forces, $\mathbf{F}_d$ as the coefficient matrix of viscous friction and $\mathbf{F}_s$ as a Coulomb friction term. $\mathbf{M}(\mathbf{x})$ denotes the mass matrix, $\mathbf{C}(\mathbf{x},\dot{\mathbf{x}})$ denotes the Coriolis/centripetal matrix, and $\mathbf{G}(\mathbf{x})$ denotes the gravity vector which are defined in previous section. $\mathbf{J}$ is the jacobian matrix of the robot and $\mathbf{T}_d$ denotes disturbance, which may represent, any modeling

uncertainty. The robot dynamics may be written as

$$\mathbf{M}(\mathbf{x})\ddot{\mathbf{x}} + \mathbf{N}(\mathbf{x},\dot{\mathbf{x}}) = -\mathbf{J}^T\boldsymbol{\tau} \tag{15}$$

where

$$\mathbf{N}(\mathbf{x},\dot{\mathbf{x}}) = \mathbf{C}(\mathbf{x},\dot{\mathbf{x}})\dot{\mathbf{x}} + \mathbf{G}(\mathbf{x}) + \mathbf{F}_d\dot{\mathbf{x}} + \mathbf{F}_s(\dot{\mathbf{x}}) + \mathbf{T}_d \tag{16}$$

It should be noted that the dynamic model is valid only when $\boldsymbol{\tau} \geq 0$ and $\mathbf{J}$ is nonsingular. On the other hand, the actuators dynamics is represented by

$$\mathbf{I}_m\ddot{\mathbf{q}} + \mathbf{D}\dot{\mathbf{q}} - r\boldsymbol{\tau} = \mathbf{u} \qquad \boldsymbol{\tau} \geq 0 \tag{17}$$

in which, $\mathbf{q}$ denotes motors angular position vector, $\mathbf{I}_m$ denotes actuator moments of inertia matrix, $\mathbf{D}$ denotes a diagonal positive definite matrix which represents actuator viscous friction, r denotes the radius of pulleys, $\boldsymbol{\tau}$ denotes the cable tension vector and $\mathbf{u}$ denotes the motor torque vector. As for the position reference, define all $\mathbf{q}$ to be zero when the end-effector centroid is located at the central position. From this configuration positive angle $\mathbf{q}$ will cause a change $\Delta\mathbf{L}$ in cable lengths, therefore, we have:

$$\Delta\mathbf{L} = r\mathbf{q} = \mathbf{L} - \mathbf{L}_0 \Rightarrow \mathbf{q} = r^{-1}(\mathbf{L} - \mathbf{L}_0) \tag{18}$$

where $\mathbf{L}_0$ is the initial length vector at $\mathbf{x} = 0$. Differentiate this equation and use manipulator Jacobian relation $\dot{\mathbf{L}} = \mathbf{J}\dot{\mathbf{x}}$ to write:

$$\dot{\mathbf{q}} = r^{-1}\dot{\mathbf{L}} = r^{-1}\mathbf{J}\dot{\mathbf{x}} \ , \ \ddot{\mathbf{q}} = r^{-1}\mathbf{J}\ddot{\mathbf{x}} + r^{-1}\dot{\mathbf{J}}\dot{\mathbf{x}} \tag{19}$$

Use Eqs. (19), (17) and (14) with some manipulations one may reach to:

$$\mathbf{M}_{eq}(\mathbf{x})\ddot{\mathbf{x}} + \mathbf{N}_{eq}(\mathbf{x},\dot{\mathbf{x}}) = \mathbf{J}^T\mathbf{u} \tag{20}$$

in which,

$$\begin{cases} \mathbf{M}_{eq}(\mathbf{x}) = r\mathbf{M}(\mathbf{x}) + r^{-1}\mathbf{J}^T\mathbf{I}_m\mathbf{J} \\ \mathbf{C}_{eq}(\mathbf{x},\dot{\mathbf{x}}) = r\mathbf{C}(\mathbf{x},\dot{\mathbf{x}}) + r^{-1}\mathbf{J}^T\mathbf{I}_m\dot{\mathbf{J}} \\ \mathbf{N}_{eq}(\mathbf{x},\dot{\mathbf{x}}) = r\mathbf{N}(\mathbf{x},\dot{\mathbf{x}}) + r^{-1}\mathbf{J}^T\mathbf{I}_m\dot{\mathbf{J}}\dot{\mathbf{x}} + r^{-1}\mathbf{J}^T\mathbf{D}\mathbf{J}\dot{\mathbf{x}} \end{cases} \tag{21}$$

In this formulation, actuator dynamics is included and transformed into task space by Jacobian matrix, which is a projection from cable length space to task space.

3 Robust PID Control of Cable Driven Robot

In this section we propose a robust PID controller based on the nominal model of the system. In the design procedure of the controller we suppose that the dynamical

matrices such as $\mathbf{M}_{eq}(\mathbf{x})$, $\mathbf{C}_{eq}(\mathbf{x},\dot{\mathbf{x}})$, etc are all uncertain and we have only some information about their bounds. Furthermore, we suppose that the end-effector position $\mathbf{x}$ is accurately measured in real time. In contrast, it is assumed that the attachment points are not precisely implemented in practice. Therefore, we have to use an uncertain jacobian matrix $\hat{\mathbf{J}}$ obtained from the uncertain installation of the attachment points. The control law is designed based on these bounds and assumptions to satisfy some robust stability conditions.

Recall the dynamic model of system (20), in presence of uncertainties in all dynamical terms, it can be shown that [15]:

$$\underline{m} \leq \|\mathbf{M}_{eq}(\mathbf{x})\| \leq \overline{m} \;\; ; \;\; \|\mathbf{C}_{eq}(\mathbf{x},\dot{\mathbf{x}})\| \leq \xi_{C_{eq}}\|\dot{\mathbf{x}}\| \tag{22}$$

$$\|\mathbf{G}_{eq}(\mathbf{x})\| \leq \xi_{g_{eq}} \;\; ; \;\; \|\mathbf{F}_d\dot{\mathbf{x}} + \mathbf{F}_s(\dot{\mathbf{x}})\| \leq \xi_{f0} + \xi_{f1}\|\dot{\mathbf{x}}\| \tag{23}$$

$$i_{m1}\mathbf{I} \leq \mathbf{I}_m \leq i_{m2}\mathbf{I} \;\; ; \;\; d_1\mathbf{I} \leq \mathbf{D} \leq d_2\mathbf{I} \tag{24}$$

in which $\underline{m}, \overline{m}, \xi_{C_{eq}}, \xi_{g_{eq}}, \xi_{f0}, \xi_{f1}, i_{m1}, i_{m2}, d_1$, and d_2 are some positive real constants. Moreover, if the disturbances are bounded, for a positive constant ξ_t one may write:

$$\|\mathbf{T}_d\| \leq \xi_t \tag{25}$$

Now choose a controller for the system consist of a PID control law and a corrective term $\mathbf{Q}$, as following:

$$\mathbf{u} = \hat{\mathbf{J}}^{\dagger}\left[\mathbf{K}_V\dot{\mathbf{e}} + \mathbf{K}_P\mathbf{e} + \mathbf{K}_I\int_0^t \mathbf{e}(s)ds\right] + r\mathbf{Q} = \hat{\mathbf{J}}^{\dagger}\mathbf{K}\mathbf{y} + r\mathbf{Q} \tag{26}$$

in which,

$$\mathbf{e} = \mathbf{x}_d - \mathbf{x} \tag{27}$$

$$\mathbf{K} = [\mathbf{K}_I \;\; \mathbf{K}_P \;\; \mathbf{K}_V] \tag{28}$$

$$\mathbf{y} = \left[\int_0^t \mathbf{e}^T(s)ds \;\; \mathbf{e}^T \;\; \dot{\mathbf{e}}^T\right]^T \tag{29}$$

and, $\hat{\mathbf{J}}^{\dagger}$ denotes the pseudo-inverse of $\hat{\mathbf{J}}^T$. In this controller structure the corrective term $\mathbf{Q}$ spans the null space of $\hat{\mathbf{J}}^T$ and must satisfy

$$\hat{\mathbf{J}}^T\mathbf{Q} = \mathbf{0} \tag{30}$$

The vector $\mathbf{Q}$ is used in the control structure to ensure that all cables remain in tension in the whole workspace. Moreover, this term increases the stiffness of the system. The estimated matrix $\hat{\mathbf{J}}^T$ obtained from inaccurate installation of the attachment points is assumed to be bounded by:

$$\|\mathbf{I} - \mathbf{J}^T\hat{\mathbf{J}}^{\dagger}\| \leq \delta_1\,, \qquad \|\mathbf{J} - \hat{\mathbf{J}}\| \leq \delta_2 \tag{31}$$

By implementation of this control law $\mathbf{u}$, in the system dynamics represented by (20), the closed loop system error dynamics may be written as:

$$\dot{\mathbf{y}} = \mathbf{A}\mathbf{y} + \mathbf{B}\Delta\mathbf{A} \tag{32}$$

in which,

$$\mathbf{A} = \begin{bmatrix} \mathbf{0} & \mathbf{I}_6 & \mathbf{0} \\ \mathbf{0} & \mathbf{0} & \mathbf{I}_6 \\ -\mathbf{M}_{eq}^{-1}\mathbf{K}_I & -\mathbf{M}_{eq}^{-1}\mathbf{K}_P & -\mathbf{M}_{eq}^{-1}\mathbf{K}_V \end{bmatrix} \ , \ \mathbf{B} = \begin{bmatrix} \mathbf{0} \\ \mathbf{0} \\ \mathbf{M}_{eq}^{-1} \end{bmatrix} \tag{33}$$

and

$$\Delta\mathbf{A} = \mathbf{N}_{eq}(\mathbf{x}, \dot{\mathbf{x}}) + \mathbf{M}_{eq}\ddot{\mathbf{x}}_d + (\mathbf{I} - \mathbf{J}^T\hat{\mathbf{J}}^{\dagger})\mathbf{u}_1 + r(\hat{\mathbf{J}}^T - \mathbf{J}^T)\mathbf{Q} \tag{34}$$

It is fully elaborated in [15], that the positioning error represented by (32) is uniformly ultimately bounded (UUB) provided that the control gains are selected from a suitable feasible set. Furthermore, it is shown that if the control gains $\mathbf{K}_P, \mathbf{K}_v$, and $\mathbf{K}_I$ are chosen large enough, the feasibility conditions are easily satisfied. The proof of these conditions are based on Lyapunov stability analysis for the uncertain system. In this paper we leave the theoretical details of the proposed method, and verify the performance of the closed-loop system through experiments.

4 Experimental Results

In order to verify the performance of the proposed method, it is applied to a planar cable robot. This manipulator consists of four actuated limbs and has with three degrees of freedom (x, y, ϕ), and is under investigation for high speed and wide workspace applications in K. N. Toosi University of Technology.

4.1 Experimental Setup

The planar cable robot under investigation is illustrated in Fig.(3), in which the end-effector mass is considered as $m = 2.5\,\text{kg}$ with a variation of $1\,\text{kg}$. Actuators are located on the vertices of a rectangle with dimension of $2.24\,\text{m} \times 2.1\,\text{m}$. The block diagram of the cable robot control hardware configuration is shown in Fig. (4), in which a real-time hardware in the loop structure is used for the experiments. The host computer serves as the user interface and enables the user to edit and modify the controller in a user friendly environment. This interface is developed in Simulink toolbox of Matlab to provide suitable environment for evaluation of different control routines on the system. The target computer is a real time processing computer which uses QNX operating system and performs real time execution of the control

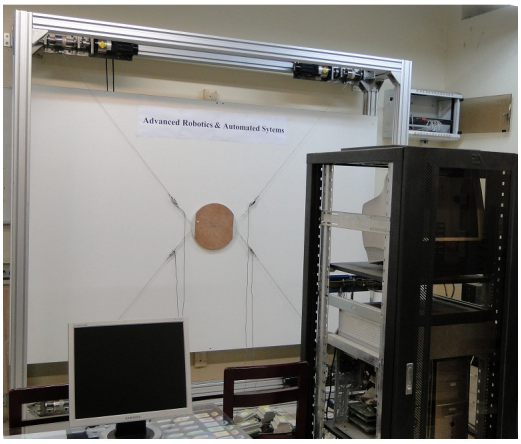

Fig. 3 The planar cable driven redundant parallel manipulator under investigation for high speed and wide workspace applications in K. N. Toosi University of Technology

laws and real time communication with Input/Output channels. RT-LAB software is used as the main hardware in the loop software and uses Simulink toolbox of Matlab to easily define the required operations and compile and execute those operations in real time QNX environment [16]. The interfacing boards between the sensors, actuators and the target computer are channeled through PCI bus I/O interfaces, and are integrated with the RT-LAB and Matlab to create a real time control system.

4.2 Control Scheme

To have a good performance in position and orientation tracking, servo drives should generate the desired tensions in the cables according to the outputs of the proposed control algorithm. In other words, the servo drives should perform as ideal torque sources to be able to perform such task. Based on this fact, cascade control scheme is proposed for the experiments. The cascade control strategy uses two control loops, called as the outer and the inner loops as shown in Fig. (5). The main goal of the outer loop which consists of the proposed PID control law is to control the position and orientation of the end-effector. Inputs of this loop are the position and orientation errors and its outputs are desired tensions in the cables. In the inner loop, the

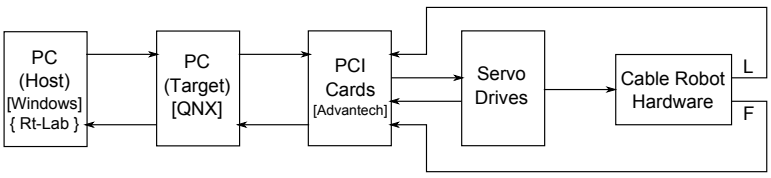

Fig. 4 Control Experimental Setup

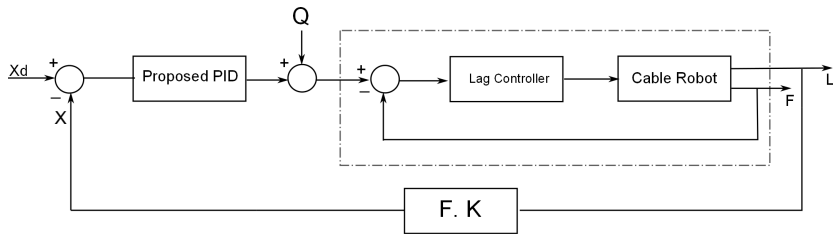

Fig. 5 Cascade control block diagram

desired tensions are compared to actual tensions measured by force sensors embedded at the end-effector attachment points. TLL500 from Transducer Techniques is used as suitable force sensors in the experiments due to their relatively large measurement range and low weight. Since in practice the actual tensions can never track the desired tensions perfectly, the main purpose of using cascade scheme in control structure of the robot is to obtain a desirable bandwidth for the inner loop which is much larger than that for the outer control loop [17]. Notice that to implement the proposed control law it is assumed that the position of the end-effector is measured in task space. However,in practice and for this experiments the cable lengths are measured in the joint space, and as shown in Fig. (5), forward kinematics solution is used to find the position vector $\mathbf{x}$. In practice, a suitable solution to forward kinematics of the robot is found in real time, by implementation of sequential quadratic programming routine (CFSQP) as an s-function in Simulink.

4.3 Results

The first set of experiments aims to generate two disjoint linear motions in translation and rotation. In x direction, it is considered to move the end-effector from the origin to $[0.2,0,0]^T$ and in ϕ direction it is considered to rotate the end-effector from its central position to $[0,0,\pi/9]^T$. Furthermore a more challenging circular profile is considered in the next experiments, to track a circular path of 0.2m about the central position. For the first experiment, suppose that the home position for the end-effector is $\mathbf{x} = [0,0,0]^T$ in SI units and the desired end-effector position and orientation is $\mathbf{x}_d = [0.2,0,0]^T$. The results of implementation using proposed PID control (26) in companion to the required $\mathbf{Q}$, which ensures that all the cables are in tension, are given in Fig. (6). The controller gains are selected in the feasible stability region of the system considering modeling uncertainty bounds, as $k_P = 500$, $k_V = 150$, $k_I = 20$. As it is seen in this figure position and orientation outputs track the desired values very well and the steady state errors are very small and in order of 10^{-3}, while as it is shown in Fig. (7) all cables are in tension for the whole maneuver. The prescribed uniformly ultimately bounded tracking error for the control structure is verified in all three directions in this experiment.

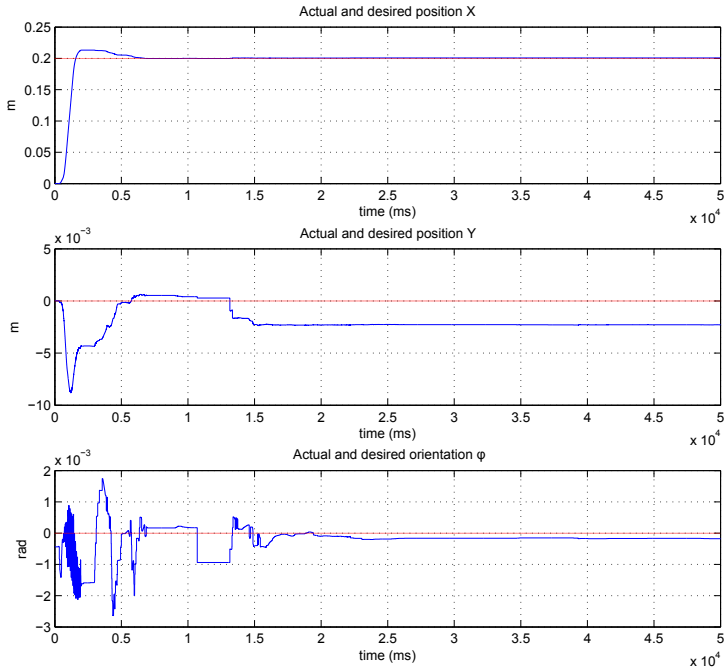

Fig. 6 Implementation results showing the actual and desired position and orientation of the end-effector for $\mathbf{x}_d = [0.2, 0, 0]^T$

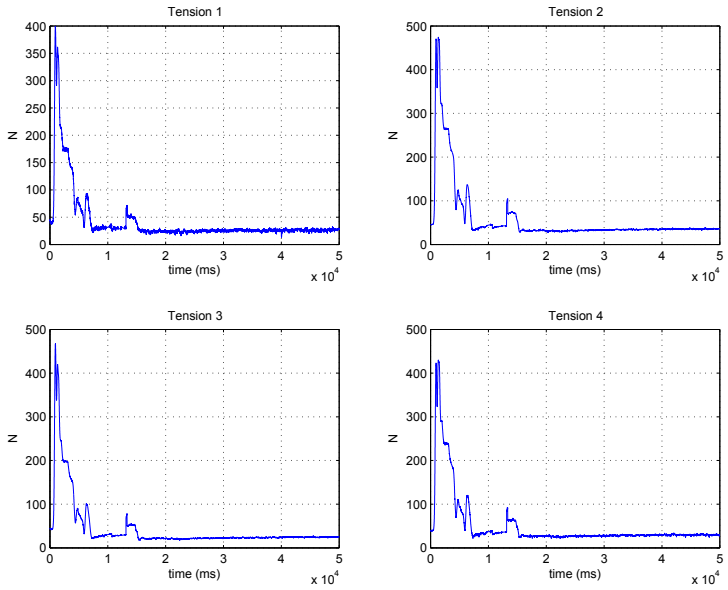

Fig. 7 Implementation results showing the cables tension for $\mathbf{x}_d = [0.2, 0, 0]^T$

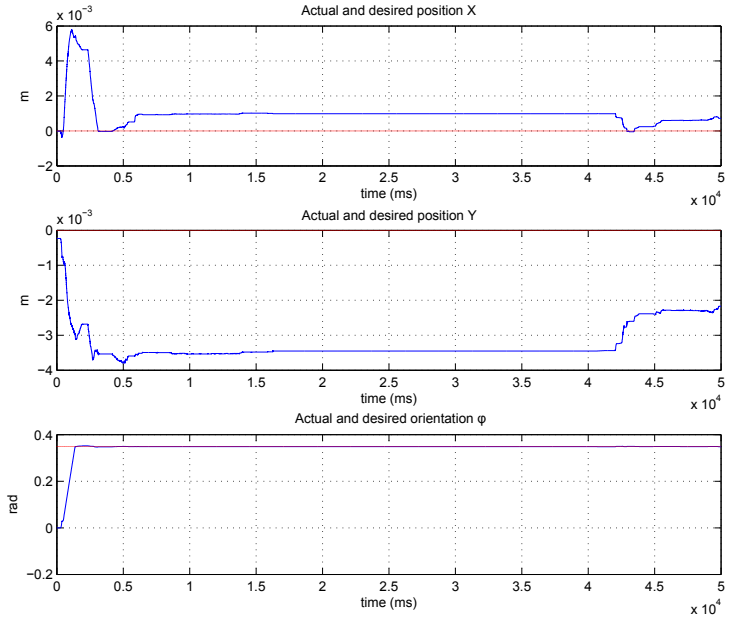

Fig. 8 Implementation results showing the actual and desired position and orientation of the end-effector for $\mathbf{x}_d = [0, 0, \pi/9]^T$

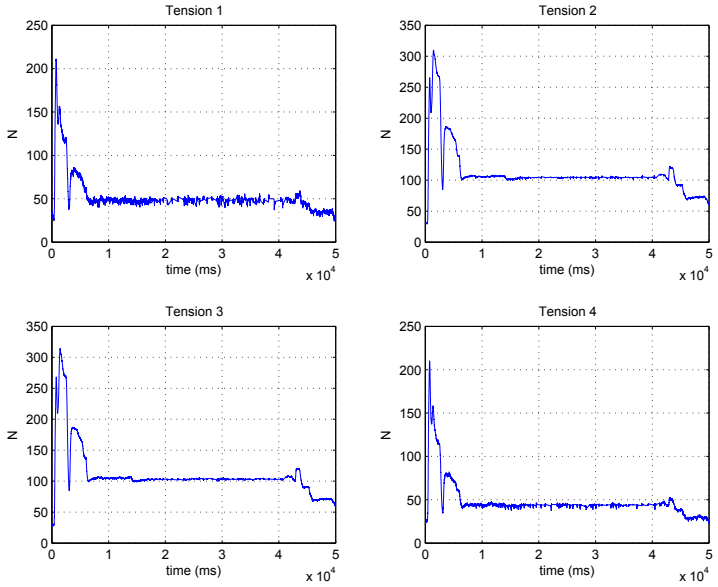

Fig. 9 Implementation results showing the cables tension for $\mathbf{x}_d = [0, 0, \pi/9]^T$

In the second experiment, suppose that the desired orientation of the end-effector is $\mathbf{x}_d = [0,0,\pi/9]^T$, while the same controller gains are considered. The experimental results are given in Fig. (8). As it is observed, tracking performance is very suitable and the position errors in x and y directions are small and in order of 10^{-3}. Furthermore, as it is shown in Fig. (9), it is observed that all tensions in the cables for this test are also positive.

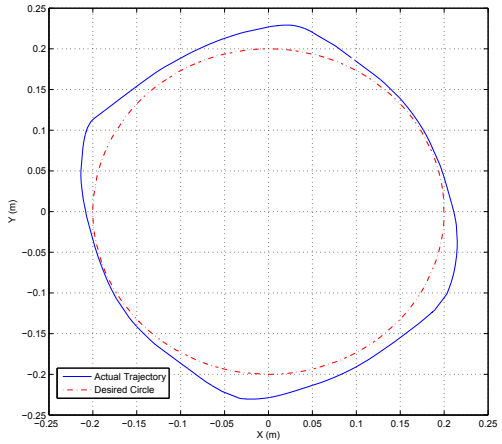

Fig. 10 Implementation results for a circular trajectory

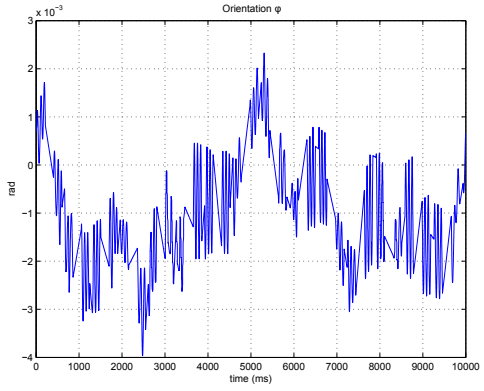

Fig. 11 Implementation results showing the rotation ϕ during circular trajectory

For the circular profile, the end-effector is commanded to track a circular path with radius of 0.2 meter in 10 seconds, while attempting to maintain $\phi = 0$ in all time. The reference Cartesian positions for this experiment are $x = 0.2\cos(0.2\pi t)$ and $y = 0.2\sin(0.2\pi t)$. Figures (10) and (11) show the reference and actual circle and deviation of ϕ from its zero desired value. It can be seen that the proposed PID control scheme is capable to perform such maneuver, while the absolute positioning

errors are relatively small. As it is seen in Fig. (11), orientation error in this test is very small and in order of 10^{-3}.

To verify the repeatability of the cable robot another experiment is performed. Repeatability of the cable robot is considered by repeating performance of a circular trajectory of the end-effector. In this experiment the trajectory is considered for eight turns, for a circle with radius of 0.2 meter, while attempting to maintain zero orientation. Figure (12) shows the performance of the robot in this experiment. As it is seen in this figure the repeatability performance of the robot is far better than absolute positing of the end effector. There are some potential sources of error in these experiments which are under current improvement. One issue is the friction and backlash in the gearing transmission of the actuators and other uncertainties that are not taken into account. Furthermore, as explained before, actual position and orientation of the end-effector are not directly measured and are computed by forward kinematics solution. This leads to a finite error in the computations which may lead to the final positioning error of the system. Furthermore, the elasticity of the cables are simply neglected in this analysis, which may lead to positioning errors, especially at high speed maneuvers.

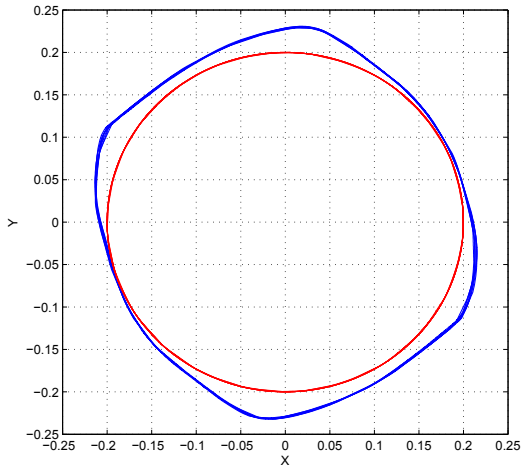

Fig. 12 Implementation results showing the repeatability of the cable robot

5 Conclusion

This paper addresses the issues of dynamic analysis and control of fully constrained cable robots. According to limiting characteristics of cables that can only apply tensile forces, and in order to ensure that all the cables are in tension for all maneuvers in their workspace, a corrective term based on null space of the Jacobian transpose is used in companion with the proposed PID algorithm. In the design of proposed

PID controller it is assumed that in dynamic equations of cable robot all terms are uncertain and only some information about their upper bounds is available. A robust PID controller is proposed to overcome partial knowledge of robot, and to guarantee boundedness of tracking errors. Finally, to show the effectiveness of the proposed algorithm several experiments on a three degrees of freedom planar cable robot are performed with different desired trajectories and suitable tracking performance for the closed loop system is reported.

References

1. Skycam, an innovative technology, *http://www.skycam.tv.* Oklahoma, USA, 2006.
2. H.D. Taghirad and M.A.Nahon, *Kinematic Analysis of A Macro–Micro Redundantly Actuated Parallel Manipulator.* Advanced Robotics, vol. 22, no. 6-7, pp. 657-87, 2008.
3. M.A. Khosravi and H.D. Taghirad, *Dynamic Analysis and Control of Cable Driven Robots with Elastic Cables.* Transactions of the Canadian Society for Mechanical Engineering, Vol. 35, No. 4, pp. 543-557, 2011.
4. R. Bostelman, J. Albus, N. Dagalakis, A. Jacoff, *Applications of the NIST Robocrane.* Proceedings of the 5^{th} International Symposium on Robotics and Manufacturing, 1994.
5. K. Maeda, S. Tadokoro, T. Takamori, M. Hiller, R. Verhoeven, *On design of a redundant wire-driven parallel robot WARP manipulator.* Proceedings of IEEE International Conference on Robotics and Automation, 1999.
6. S. Kawamura, H. Kino, C. Won, *High-speed manipulation by using parallel wire-driven robots.* Robotica, Vol. 18, No. 3, pp. 13-21, 2000.
7. R. Roberts, T. Graham, T. Lippitt, *On the Inverse Kinematics, Statics, and Fault Tolerance of Cable-Suspended Robots.* Journal of Robotic Systems, Vol. 15, No. 10, pp. 649-661, 1998.
8. A. Riechel, P. Bosscher, H. Lipkin, I. Ebert-Uphoff, *Cable Driven Robots for Use in Hazardous Environments.* Proceedings of 10^{th} International Conference on Robotics and Remote systems for Hazardeous Enviromnments, Gainesville, 2004.
9. S. Behzadipour, A. Khajepour, *Stiffness of Cable-based Parallel Manipulators With Application to Stability Analysis.*, Journal of Mechanical Design, Vol. 128, No. 1, pp. 303310, 2006.
10. A. Alp, S. Agrawal, *Cable Suspended Robots: Feedback Controllers with Positive Inputs.* Proceedings of the American Control Conference, 2002.
11. R.L. Williams, P. Gallina and J. Vadia, *Planar Translational Cable Direct Driven Robots.*, Journal of Robotic Systems, Vol. 20, No. 3, pp. 107-120, 2003.
12. S. Ryoek and S. Agrawal, *Generation of Feasible Set Points and Control of a Cable Robot.*, IEEE Tran. on Robotics, Vol. 22, No. 3, pp. 551-558, 2006.
13. H. Kino, T. Yahiro, F. Takemura, *Robust PD Control Using Adaptive Compensation for Completely Restrained Parallel-Wire Driven Robots.* IEEE Trans. on Robotics, Vol. 23, No. 4, 2007.
14. X. Diao, O. Ma, *Vibration analysis of cable-driven parallel manipulators.*, Multibody Syst Dyn, 21: 347–360, 2009.
15. M.A. Khosravi and H.D. Taghirad, *Robust PID Control of Fully-Constrained Cable Driven Robots.*, submitted to IEEE/ASME Trans. on Mechatronics, 2012.
16. *RT-LAB version 8 User Guide.*, Opal-RT Company, 2005.
17. G. Meunier, B. Boulet, M. Nahon, *Control of an Overactuated Cable-Driven Parallel Mechanism for a Radio Telescope Application.*, IEEE Tran. On Control Systems Tech., Vol. 17, No. 5, pp. 1043-1054, 2009.